Nat Comput (2013) 12:259–276
DOI 10.1007/s11047-012-9357-2

Cooperative linear cargo transport with molecular spiders

Oleg Semenov · Mark J. Olah · Darko Stefanovic

Published online: 9 November 2012

Abstract Molecular spiders are nanoscale walkers made with DNA enzyme legs attached to a common body. They move over a surface of DNA substrates, cleaving them and leaving behind product DNA strands, which they are able to revisit. Simple one-dimensional models of spider motion show significant superdiffusive motion when the leg-substrate bindings are longer-lived than the leg-product bindings. This gives the spiders potential as a faster-than-diffusion transport mechanism. However, analysis shows that single-spider motion eventually decays into an ordinary diffusive motion, owing to the ever increasing size of the region of cleaved products. Inspired by cooperative behavior of natural molecular walkers, we propose a symmetric exclusion process model for multiple walkers interacting as they move over a one-dimensional lattice. We show that when walkers are sequentially released from the origin, the collective effect is to prevent the leading walkers from moving too far backwards. Hence, there is an effective outward pressure on the leading walkers that keeps them moving superdiffusively for longer times, despite the growth of the product region. Multi-spider systems move faster and farther than single spiders or systems with multiple simple random walkers.

Keywords Molecular spider · Multiple random walkers · Symmetric exclusion process · DNA walker · Deoxyribozyme

O. Semenov · M. J. Olah · D. Stefanovic (✉)
Department of Computer Science, University of New Mexico, Albuquerque, USA
e-mail: darko@cs.unm.edu

D. Stefanovic
Center for Biomedical Engineering, University of New Mexico, Albuquerque, USA

1 Introduction

Molecular walkers (or, molecular motors) are natural or synthetic molecules that move over surfaces or along tracks or fibers. Their motion is propelled by the energy released by a succession of chemical reactions that take place as the walkers bind and release their legs; the energy is supplied by other molecules, either from the walking surface itself or from the surrounding solution. Molecular walkers provide a means to transport material by non-diffusive directed motion. Molecular walkers are ubiquitous as a transport mechanism in biological systems (Schliwa and Woehlke 2003), and many of the complex regulatory cellular processes are controlled by the action of molecular walkers such as kinesin and dynein (Hirokawa and Takemura 2005). It has been demonstrated experimentally that these natural cellular molecular walkers work in teams, wherein their collective action leads to behaviors not possible for a single walker (Badoual et al. 2002). In addition, theoretical models predict that collective cooperative or competitive behavior of walkers is fundamentally different from the behavior of individual walkers (Campas et al. 2006; Frey et al. 2004; Jülicher et al. 1997).

Inspired by the potential for walker cooperation, we propose a model describing the collective behavior of teams of molecular walkers.[1] Our model is based on synthetic walkers called *molecular spiders* (Pei et al. 2006) (Sect. 2). Figure 1 shows a molecular spider walking over a surface displaying *substrate* molecules. A molecular spider has two or more enzymatic legs attached to a common

[1] A preliminary report on this research was presented at the 17th International Conference on DNA Computing and Molecular Programming (Semenov et al. 2011).

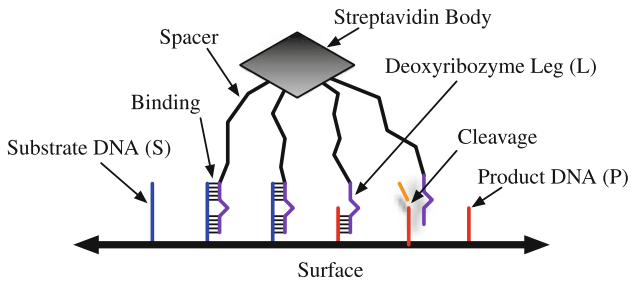

Fig. 1 A molecular spider is a streptavidin-bodied molecular walker that moves over a surface of single-stranded DNA substrates. It has several flexible deoxyribozyme legs that attach to, cleave, and detach from the DNA substrates. Cleavage leaves behind shorter product DNA strands that can still be re-bound by legs, but less strongly (Not to scale.)

body. The legs are deoxyribozymes—catalytic sequences of single-stranded DNA that can cleave complementary single-stranded DNA *substrates*. A spider moves over the surface, attaching to, cleaving, and detaching from the substrate sites. It leaves behind *product* DNA strands, which are the surface-bound portions of the cleaved substrates. Experiments have shown that this mechanism allows spiders to move directionally over nanoscale tracks of regularly spaced DNA substrates (Lund et al. 2010).

Antal and Krapivsky proposed a simple abstract model that describes molecular spider motion in one dimension (1D) as a continuous-time Markov process (Antal and Krapivsky 2007; Antal et al. 2007). In previous work, we showed via computer simulation and analytical arguments that walkers in the Antal–Krapivsky (AK) model move superdiffusively over significant times and distances (Semenov et al. 2011), and hence are useful as a faster-than-diffusion molecular transport mechanism. However, in the asymptotic limit of long times, the AK walkers slow down and move as an ordinary diffusive process (Antal and Krapivsky 2007). This can be explained by understanding that superdiffusion is only possible while there is an energy source available to bias the motion of a spider. In the AK model, the energy is provided by the irreversible transformation of substrates into products. This is manifested as a difference in residence times between substrate and product attachments. When a spider is attached to products, there is no energy available to it, and its motion is unbiased and diffusive. When a spider is attached to a substrate, the slower rate of catalysis creates a bias that makes it more likely for the spider to move to new, unvisited substrate sites. However, as a spider moves, it cleaves out an increasingly large region of products called the *product sea*. As the product sea grows, the spider spends increasingly more time diffusing through it, and less time cleaving new substrate sites. Hence, the spider's motion asymptotically decays to ordinary diffusion.

In this work, we started with the hypothesis that the collective action of many spider walkers could lead to cooperative behavior that would enhance the superdiffusive motion of the spiders close to the boundary. The simplicity of the AK model and the known results for single walker motion make it a particularly useful model for extension to the study of collective spider motion. The AK model contains only those features and properties necessary to explain superdiffusive motion of (single) spiders, abstracting away the extraneous details of the specific spider chemistry and focusing on the kinetics of nearest-neighbor walking gaits for multipedal enzymatic walkers. We extend these nearest-neighbor walking gaits to collective motion of spiders in 1D. An immediate consequence is that AK spiders cannot move past one another, as their legs are too short to hop over adjacent walkers. As a result even if the product sea becomes very large, a spider near the boundary of the sea cannot move further back than the next spider behind it. Hence by adding spiders at the origin the effective size of the product sea as seen by the leading spiders is reduced. In essence, the presence of other spiders can act as an exclusionary pressure that enhances transport of cargo carried by the leading spiders. Ideally the leading spider would perceive a constant-size sea of products behind it, and its diffusive excursions into that sea would be of constant duration, which would lead to asymptotically superdiffusive motion.

In Sect. 3 we present a model for cooperative multi-spider transport over an infinite 1D lattice. The model relies on an unlimited supply of identical new spiders injected at the origin whenever the sites at the origin are unoccupied. Conceptually this spider injection approximates the release of spiders from a large reservoir near the origin. Using Kinetic Monte Carlo (KMC) methods, we show that multi-spider systems exhibit significantly super diffusive motion within the time bounds studied (Sect. 4), with both the duration of the superdiffusive period and the peak superdiffusivity coefficient greater than for single walkers (Sect. 4.2). This shows potential for multi-spider systems with injection to be used to perform useful tasks in nanoscale computational and communication systems by providing a faster-than-diffusion mechanism of "first-to-target" transport.

However, even with an unbounded reservoir of new spiders, the *asymptotic* behavior of the leading spider is still ordinary-diffusive, not superdiffusive! Sects. 5, 6, 7 explain this result by investigating the effective size of the product sea, the number of injected spiders, and the spatial distribution of spiders. Importantly, we find that even though the multi-spider model is not asymptotically super diffusive, it still has superior transport properties. Indeed, the multipedal nature of spiders has quantifiable advantages over systems of interacting simple random walkers (i.e., spiders with just one leg). In analogy to the bipedal walkers, ubiquitous in natural systems, multipedal walkers

present distinct advantages for molecular transport, whether acting alone or as part of a collective.

2 Molecular spiders

A molecular spider (Fig. 1) has a rigid, chemically inert body (such as streptavidin) and several flexible legs made of deoxyribozymes—enzymatic single-stranded DNA that can bind to and cleave complementary strands of a DNA substrate at the point of a designed ribonucleic base impurity. When a spider is placed on a surface on which the appropriate DNA substrate has been deposited (or nanoassembled), the legs bind to the substrate and catalyze its cleavage, creating two product strands. The upper portion floats away in solution and we do not consider it further. The lower portion remains on the surface, and, because it is complementary to the lower part of the leg, there is some residual binding of the leg to the product, typically much weaker and shorter-lived than the leg-substrate binding. The leg kinetics are described by the five reactions in Eq. 1 relating legs (L), substrates (S), and products (P), in which we have folded the catalysis reaction and subsequent dissociation reactions into a single k_{cat} rate:

$$\mathrm{L} + \mathrm{S} \underset{k_{\mathrm{S}}^{-}}{\overset{k_{\mathrm{S}}^{+}}{\rightleftarrows}} \mathrm{LS} \overset{k_{\mathrm{cat}}}{\rightarrow} \mathrm{L} + \mathrm{P} \tag{1}$$

$$\mathrm{L} + \mathrm{P} \underset{k_{\mathrm{P}}^{-}}{\overset{k_{\mathrm{P}}^{+}}{\rightleftarrows}} \mathrm{LP} \tag{2}$$

2.1 The Antal–Krapivsky model

The Antal–Krapivsky model (Antal and Krapivsky 2007; Antal et al. 2007) is a high-level abstraction that represents a molecular spider as a random walker. Unlike ordinary random walkers, each AK spider has k legs. The chemical activity of the multiple legs is independent, but their motion is constrained by their attachment to a common body; in the model, any two legs must be within distance s. The legs walk over sites on a regular 1D lattice, where each site is either a substrate or a product.

Mathematically, the AK model takes the form of a continuous-time Markov process. The system states of this process are given by the combined state of the lattice sites and the state of the spider legs. All lattice sites are initially substrates and are only transformed to products when a leg detaches from the substrate (via catalysis). Thus the state of the lattice sites is fully described by the set $P \subset \mathbb{Z}$ of product sites. The state of the spider is completely defined by the set F of attached feet locations. Thus any state can be described as the pair (P, F).

2.1.1 Spider gait

We call F a *configuration* of the legs. The *gait* of a spider is defined by what configurations and what transitions between configurations are allowed in the model. In any state $(P, F) \in \Omega$ where Ω is a state space of the Markov process, all k legs are attached. Together with the restriction that at most one leg may be attached to a site, this implies that

$$|F| = k. \tag{3}$$

Additionally, the legs are constrained by their attachment to a common body. If the spider has a point body with flexible, string-like legs of length $s/2$, then any two feet can be separated by at most distance s, thus,

$$\max(F) - \min(F) \leq s. \tag{4}$$

The transitions in the spider Markov process correspond to individual legs unbinding and rebinding. When a spider is in configuration F, any foot $i \in F$ can unbind and move to a nearest-neighbor site $j \in \{i+1, i-1\}$ to form a new configuration $F' = (F \setminus \{i\}) \cup \{j\}$, provided the new configuration does not violate one of the constraints of Eqs. 3 and 4. A transition $i \rightarrow j$ is called *feasible* if it meets these constraints. The feasible transitions determine the gait of the spider. The nearest-neighbor hopping combined with the mutual exclusion of legs leads to a shuffling gait, wherein legs can slide left or right if there is a free site, but legs can never move over each other, and a leg with both neighboring sites occupied cannot move at all. If the legs of such a spider were distinguishable, they would always remain in the same left-to-right ordering.

In the case where $k = 2$, $s = 2$ the gait of the spider is particularly simple (Fig. 2), but it still exhibits constraints on the coordination of the leg motion that are not present for $k = 1$ walkers.

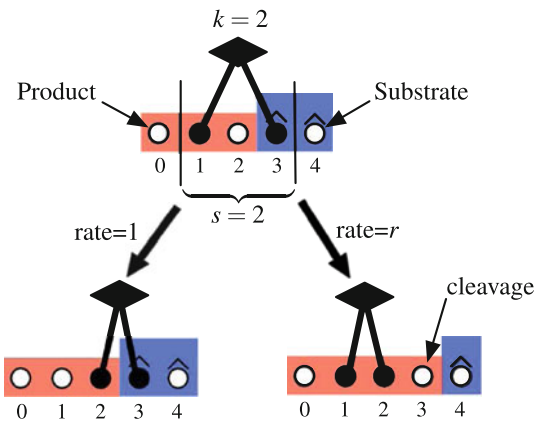

Fig. 2 An AK spider with two legs ($k = 2$) and maximum leg spacing $s = 2$ is attached to a product at site 1 and a substrate at site 3. It can detach from the product at rate 1, after which it can only move to site 2 without violating Eq. 4. Alternatively it can cleave and detach from site 3 at rate r, after which it must move to site 2

2.1.2 Transition rates

The rate at which feasible transitions take place depends on the state of the site i. If i is a product, the transition rate is 1, but if i is a substrate, the transition occurs at a slower rate $r < 1$. This is meant to model the realistically slower dissociation rates from substrates, corresponding to chemical kinetics where $k_{\text{cat}}/k_{\text{P}}^{-} = r < 1$. The effect of substrate cleavage is also captured in the transition rules. If for state (P, F), where $i \in F \setminus P$, the process makes the feasible transition $i \to j$, then the leg will cleave site i before leaving, and the new state will have $P' = P \cup \{i\}$.

The relation of the AK model to the chemistry of the spiders in Eq. 1 can be understood if one assumes the chemical rates are given as in Eq. 5:

$$\begin{aligned} k_{\text{S}}^{+} &= k_{\text{P}}^{+} = \infty \\ k_{\text{S}}^{-} &= 0 \\ k_{\text{P}}^{-} &= 1 \\ k_{\text{cat}} &= r < 1 \end{aligned} \tag{5}$$

The infinitely fast on-rates account for all legs always being attached; when a leg unbinds it instantly rebinds to some neighboring site. Thus the spider is modeled as jumping from configuration F to configuration F'.

2.2 Superdiffusive motion of single AK spiders

To characterize the motion of spiders we use the notion of *superdiffusion*. Superdiffusive motion can be quantified by analyzing the mean squared displacement (MSD) of a spider as a function of time. For diffusion in a one-dimensional space with diffusion constant D, the mean squared displacement is given by Eq. 6.

$$\text{msd}(t) = \left\langle x^2(t) \right\rangle = 2Dt^{\alpha} \begin{cases} \alpha = 0 & \text{stationary} \\ 0 < \alpha < 1 & \text{subdiffusive} \\ \alpha = 1 & \text{diffusive} \\ 1 < \alpha < 2 & \text{superdiffusive} \\ \alpha = 2 & \text{ballistic or linear} \end{cases} \tag{6}$$

We say that the spider is moving *instantaneously superdiffusively* (Lacasta et al. 2004) at a given time t if

$$\alpha(t) = \frac{d(\ln(\text{msd}(t)))}{d(\ln(t))} > 1. \tag{7}$$

Using Kinetic Monte Carlo simulations (Bortz et al. 1975) of the Markov process we can estimate the msd(t) for the spider process for different parameter values by averaging over many realizations $x(t)$ of the process $X(t)$, where each $x(t)$ is a function from $t \in [0, t_{\max}]$ to the state space Ω of the spider process, and $x(t) \sim X(t)$.

When the rate of substrate cleavage is slower than the rate of product detachment ($r < 1$), each spider process goes through three different phases of motion defined by their instantaneous value for the exponent α of msd(t). Initially spiders are at the origin and must wait for both legs to cleave a substrate before they start moving at all, so when $t < 1/r$ the process is essentially stationary; we call this largely unimportant phase the *initial phase*. After the spiders take several steps, spiders with $r < 1$ show a sustained period of superdiffusive motion over many decades in time. We call this the *superdiffusive phase*, and define it as the period during which the instantaneous estimate of $\alpha > 1.1$. The cutoff of $\alpha = 1.1$ is somewhat arbitrary but represents a threshold where spiders are moving significantly superdiffusively, in contrast to spiders with $r = 1$, which never have $\alpha > 1$. Finally, Antal and Krapivsky showed that as time goes to infinity, all spiders will approach ordinary diffusion with $\alpha \approx 1$. This final stage is called the *diffusive phase* and is characterized by spiders mainly moving over regions of previously cleaved products, which makes the values of r irrelevant, since all spiders move with rate 1 over product sites.

2.2.1 The boundary and diffusive metastates

To explain this behavior we observe that spiders with $s = 2$ and $k = 2$ always cleave all sites they move over since the AK model does not permit legs to change their effective ordering on the surface. Hence, the spiders move with a shuffling gait, consuming all products in the region they move over. This leads to the formation of a sharp boundary between a contiguous region of products called the *product sea*, and the remainder of the unvisited sites which are still substrates. The product sea has left and right boundaries defined as

$$b_R = \max(P) + 1, \text{ and, } b_L = \min(P) - 1. \tag{8}$$

Hence the sites b_R and b_L are substrates, and moreover, they are the only substrates a spider with $k = 2$, $s = 2$ can reach.

Given this definition of boundary, we can consider the spider Markov process as moving between two metastates. If the state of the system is $X = (P, F)$, then if $b_R \in F$ or $b_L \in F$, we say the system is in the *boundary* metastate ($X \in B$), otherwise the system is in the *diffusive* metastate ($X \in D$). When the system is in the B metastate, the spider moves ballistically towards unvisited sites; when it is in the D state, the spider's motion is ordinary diffusive. We define a *B-period* as an interval of time during which the spider is in the B state and a *D-period* as an interval of time during which the spider is in the D state. A realization of the spider process alternates between B- and D-periods. We define the distribution of the durations of B-periods that

begin at time t as $\tau_B(t)$, and the distribution of durations of D-periods beginning at t as $\tau_D(t)$

The transitions from the B state to D state are independent of the previous state of the system before it entered the B state, hence $\langle \tau_B(t) \rangle$ is independent of time. However, the transitions from the D state back to the B state depend on the size of the product sea that the spider has left behind, and this size increases with time. Correspondingly, it has been shown that $\langle \tau_D(t) \rangle = \Theta(\sqrt{t})$ (Semenov et al. 2011).

This explains the transient superdiffusion at short times when the spider spends more time in the B state, and the decay to ordinary diffusion at long times, as the spider spends more and more of its time in the D state.

There are two options to increase the superdiffusive effect of the spider motion: (1) decrease the effective size of the product sea, and hence the time needed to escape from it and return to the boundary ($\langle \tau_D(t) \rangle$); or (2) decrease the rate at which spiders leave the boundary. Here we focus on option (1), by means of localized release of spiders at the origin, which effectively fills the product sea with follower spiders, preventing the leading spiders from moving as far backwards away from the boundary. This works because spider legs cannot occupy the same site at the same time, and spiders walk with a shuffling gait, sliding left or right one site at a time, so a spider cannot jump over an adjacent spider. The presence of multiple spiders will restrict the motion of the spiders around them, reducing the effective size of the product sea as seen by a walker at the boundary. By releasing many spiders sequentially at the origin we make the D state of the leading spiders shorter. Ideally, we might desire to make the duration of each diffusive excursion of the leading spider independent of the number of sites that have already been cleaved (i.e. $\langle \tau_D(t) \rangle = \mathcal{O}(1)$). Such a system would have the potential for asymptotically superdiffusive motion, but it will turn out that this is not achieved in the multi-spider injection model.

3 The multi-spider model

Cooperative and interactive behavior of spiders can be studied by extending the AK model to a *multi-spider* model that describes a system of $S \geq 2$ spiders moving simultaneously. Every spider in the multi-spider model has identical values for parameters k (the number of legs) and s (the maximum leg spacing), and they all move over the same 1D surface of substrates. The (otherwise indistinguishable) spiders are enumerated as $1, \ldots, S$, which allows the state of the system to be described as

$$X = (P, F_1, \ldots, F_S). \tag{9}$$

Here, $F_i \subset \mathbb{Z}$ gives the attached leg locations of spider i. In analogy to Eqs. 3 and 4, we maintain for all i that

$$|F_i| = k \tag{10}$$

and

$$\max(F_i) - \min(F_i) \leq s. \tag{11}$$

To extend the chemical exclusionary properties of spider legs to multi-spider systems, we add the restriction that any site on the surface can be occupied by only one leg of any spider, so that for all i, j:

$$F_i \cap F_j = \emptyset. \tag{12}$$

Finally, we define a mechanism to allow the addition of new spiders into the system, allowing S to grow with time, while maintaining the Markovian properties of the process. New spiders can be added at an injection site $I = \{0,1\}$ for any state in which the sites 0 and 1 are unoccupied. A new spider is added as a Poisson process with rate $\lambda > 0$, and the initial state of the new spider is $F_{S+1} = \{0,1\}$. In the limit when $\lambda = \infty$, a new spider is added as soon as the injection site is unoccupied. Even in this limiting case, the presence of other spiders at the injection site and their finite rate of movement out of this site constrain the multi-spider system to a finite number of spiders at all times.

3.1 Rebinding gait

With multiple spiders on a lattice, there are situations where a particular spider is completely blocked from movement. This happens when its legs are together (i.e., on adjacent sites) and other spiders occupy the sites to its immediate left and right. Thus, to simplify the Markov process description, we introduce a slight change to the gait of the walker. When a leg detaches from a site i it can move not only to sites $i - 1$ and $i + 1$ as in the AK model, but also back to site i. It chooses from any site in $\{i - 1, i, i + 1\}$ with equal probability, provided none of the new configurations violates the constraints of Eqs. 10, 11, and 12. Thus, even if sites $i - 1$ and $i + 1$ are occupied, the leg has somewhere to go. We call this new spider gait the *rebinding gait*. It ensures that the probability that any particular leg will move is independent of the state of the rest of legs in the system, which simplifies the Monte Carlo simulation of the system.

Furthermore, the rebinding gait is more chemically realistic, as the enzymatic leg of a real molecular spider can always rebind to the site it just dissociated from, and its detachment should be independent of the state of the rest of the system.

From an analytical perspective, the effect of allowing rebinding is to slow the movement of walkers because of the potential for dissociations that do not move a spider leg. However, simulation results extended to very long times (Fig. 3) show that this change in effective rates does not

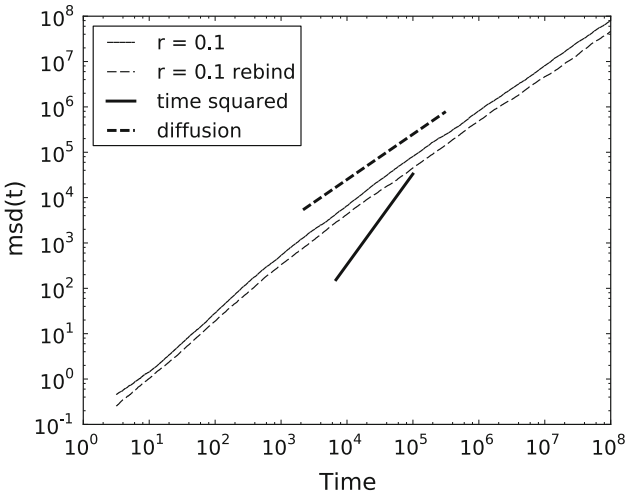

Fig. 3 Estimate of msd(t) for spiders with the AK gait and the rebinding gait with $k = 2$, $s = 2$, and $r = 0.1$

qualitatively change the motion of a single spider. The rebinding gait leads to a constant-factor decrease in the mean squared displacement. In the remainder of the paper when comparisons of multi-spider systems with rebinding gait are made with single-spider systems, the single-spider systems have the normal AK gait, without rebinding. This gives them a constant factor advantage; however, as will be seen, even with this handicap the multi-spider systems are superior as transport devices.

4 Simulation results for the multi-spider model

The multi-spider system provides a simple model for cooperative transport using interacting walkers. In this application, walkers start at the origin of a 1D surface covered with energy-supplying substrate. The walkers move outwards in the plus and minus directions consuming substrate to bias their motion outwards, leaving an ever increasing sea of products ($P \subset \mathbb{Z}$) in between the farthest sites visited in the plus and minus directions. Because spiders always cleave substrates when they detach from a site, and the spiders with $s = 2$, $k = 2$ have a shuffling gait wherein they cannot hop over any substrates, the sea of products P is always contiguous and includes the origin. Thus, as explained in Sect. 2.2.1, there is a well defined concept of a left (b_L) and right (b_R) boundary between the product sea and the unvisited substrates.

In the multi-spider model, the spiders fill this product sea, creating an exclusionary pressure that prevents the outermost spiders from moving past them. At any given time there will be one leftmost $1 \leq L_s \leq S$ and one rightmost spider $1 \leq R_s \leq S$. We are interested in the location of these leading L_s and R_s spiders as the system evolves.

When the Markov process is in state X as given by Eq. 9, the ith spider's position is defined as the mean of F_i. We use a function μ to describe the position of any spider $1 \leq i \leq S$ as

$$\mu(i) = \frac{\sum F_i}{k}. \tag{13}$$

Note that when $k = 2$, $s = 2$ as in the multi-spider model, $\mu(i)$ only takes on half-integer values and the value of $\mu(i)$ uniquely determines the value of F_i. This is in general not the case for larger values of k and s.

It is sometimes possible for the identities of the leftmost or rightmost spider to change. When $\mu(L_s) > 2$, all the spiders are to the right of the injection point $I = \{0, 1\}$, and when $\mu(R_s) < 0.5$, all the spiders are to the left of I. In these cases, when a new spider is injected at I, it becomes the new L_s or R_s, respectively. This situation becomes very unlikely as the number of spiders released increases; however, when reporting the MSD of L_s and R_s, these identity changes are important and are accounted for in our analysis.

4.1 Experimental setup

To quantify the transport characteristics of the multi-spider injection system, we define a multi-spider system that begins with two spiders on either side of an injection site near the origin. The two initial spiders start on the boundary on either side of an initial product sea (Fig. 4). The precise parameters studied are given in Table 1.

We use the Kinetic Monte Carlo (KMC) method (Bortz et al. 1975) to numerically sample traces of the multi-spider Markov process. In Table 2 we show the number of runs of the Markov process sampled for each r value and the minimum time each sample was run until.

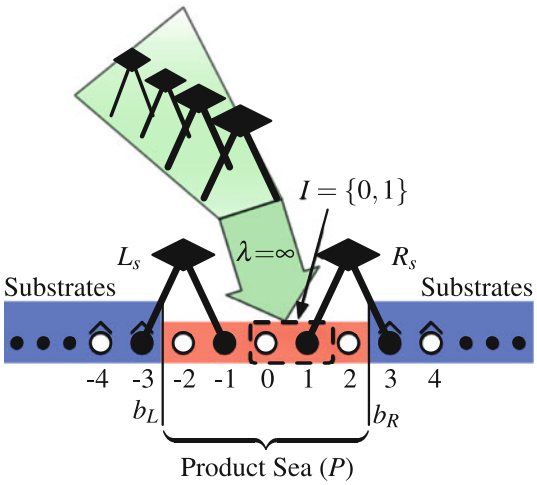

Fig. 4 The initial configuration used for the multi-spider model simulations

Table 1 Parameters studied for the multi-spider model

Parameter	Description
$k = 2$	Number of legs
$s = 2$	Maximum leg separation
$P = \{-2, -1, 0, 1, 2\}$	Initial product sea
$S = 2$	Iinitial number of spiders
$F_1 = \{1, 3\}$	Initial location of rightmost spider
$F_2 = \{-3, -1\}$	Initial location of leftmost spider
$I = \{0, 1\}$	Injection site
$\lambda = \infty$	Injection rate
$k_P^- = 1$	Rate of detachment from products
$k_{cat} = r \leq 1$	Rate of detachment from substrates

Table 2 Number of KMC runs for each parameter value and minimum simulation time combination

t_{max}	r-value					
	1.0	0.5	0.1	0.05	0.01	0.005
1.0×10^7	1,800	1,800	1,800	1,800	1,800	1,800
1.0×10^8	200	–	200	–	–	–

The primary parameter of interest is the chemical kinetics parameter r. When $r = 1$ there is no effective chemical difference between substrates and products, and hence no energy is available in the substrates to bias the outermost spiders' motion. When $r < 1$ the chemical difference at the boundary acts to bias the motion of the leftmost spider (L_s) and the rightmost spider (R_s) away from the origin when they are at their respective boundaries. This creates effective superdiffusion for the leading spiders as long as they stay near the boundary.

Table 2 shows that we have many fewer simulation traces for $t_{max} = 10^8$ than for $t_{max} = 10^7$. Indeed, these simulation counts are far fewer than the 5,000 traces computed for the single spider model (Semenov et al. 2011). We were not able to compute more traces because simulation of the multi-spider model requires much more computational resources for large values of t_{max} near 10^8. Our KMC simulations of the spider systems consist of iterative computation of consecutive discrete events of the underlying Markov process. Every individual event takes a constant amount of computational (wall) time, but the simulation time intervals between events are exponentially distributed based on the total rate of all potential transitions from the current state. There are two possible transitions from every state of the single spider model: the left leg moves, or the right leg moves. Thus, the mean simulation time duration between events remains within 1/2 and $1/(1 + r)$ for every simulated step. Since r is a constant that does not depend on t_{max}, the execution time of our single spider KMC algorithm is $O(t_{max})$, i.e., it depends linearly on the simulation time. However, in the multiple spider model the mean duration between events is not constant. When new spiders are injected, the number of different possible events in the system increases, and so the simulation time intervals between those events become smaller. Thus, to achieve desired maximum simulation time t_{max} for the multi-spiders model, we need to simulate more discrete events than for the single spider model. In Sect. 5.2 we estimate that the number of released spiders grows as $\mathcal{O}(\sqrt{t})$. Hence, the execution time of the multi-spider KMC simulation algorithm is $\mathcal{O}({t_{max}}^{3/2})$.

4.1.1 *Observed superdiffusion of the leading spiders*

As discussed in Sect. 2.2, single spider systems with $r < 1$ show transient superdiffusive behavior (Semenov et al. 2011). Single spiders move faster than ordinary diffusion for a significant time and distance, but eventually slow down and move as an ordinary diffusion. Hence, the leading spiders (L_s and R_s) of the multi-spider model also should move superdiffusively when they are near the boundary. This can be quantified by estimating the mean squared displacement of the leading spiders in the multi-spider model. Because the environment and the walker are symmetrical, we can, without loss of generality, represent the mean squared displacement of the outermost walkers by the position of the rightmost spider,

$$\text{msd}(t) = \langle \mu(R_s)(t) \rangle. \tag{14}$$

Figure 5 shows the KMC simulation estimate of msd(t) for the multi-spider model on a log–log plot for each measured r parameter value. In this plot, straight lines correspond to power laws, that is, to Eq. 6, and the parameter α is given by the slope. To show the instantaneous value of α, we use finite difference methods to estimate $\alpha(t)$ as in Eq. 7. Figure 6 shows the result of using the Savitzky–Golay smoothing filter (Press et al. 2002) on these estimates of $\alpha(t)$.

These results show the same three-phase behavior as observed in single spider simulations (Sect. 2.2). The phases can be observed by noting the estimate of the value of $\alpha(t)$ in relation to the horizontal line in Fig. 6 representing $\alpha(t) = 1.0$. Below this line, the leading spiders are moving subdiffusively and above this line the leading spiders are moving superdiffusively. For each value of r, the systems exhibit the following three sequential phases:

1. The *initial* phase is defined when $t < 1/r$. At these times, very few steps have been made, and the value of $\alpha(t)$ is largely dependent on peculiarities of the initial configuration, and not of relevance to transport phenomena.

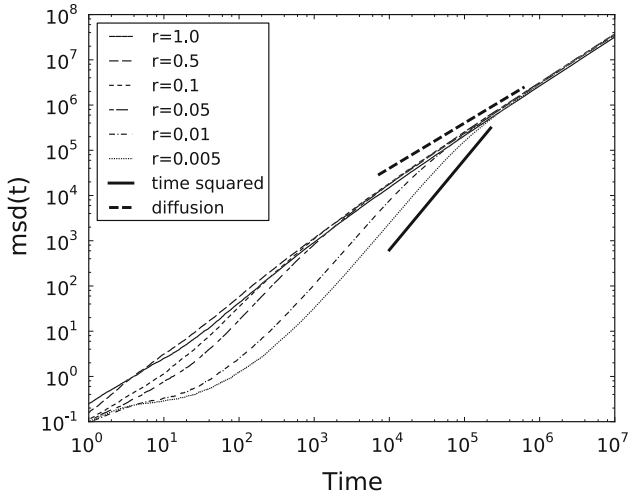

Fig. 5 Mean squared displacement for R_s. *Reference lines* are shown for ordinary diffusion and ballistic motion

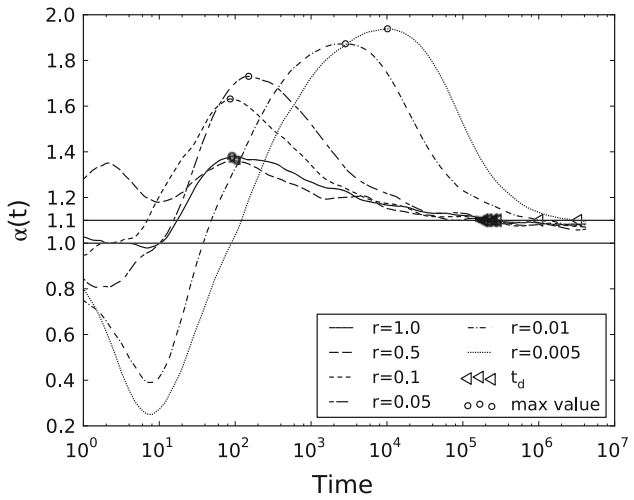

Fig. 6 Smoothed finite difference approximation of $\alpha(t)$ for R_s. *Horizontal lines* define the threshold for ordinary diffusion at $\alpha = 1.0$ and our defined threshold for superdiffusion at $\alpha = 1.1$

2. The *superdiffusive* phase begins when $t > 1/r$ and continues while the $\alpha(t) \geq 1.1$. During this phase the spiders move significantly faster than diffusion. Decreasing values of r lead to increasing maximum values of $\alpha(t)$, and a longer time until the spider returns to the $\alpha(t) = 1.1$ threshold.
3. The *diffusive* phase begins when the instantaneous value of $\alpha(t) = 1.1$, and continues indefinitely, as even the leading spiders eventually spend almost all of their time diffusing over the products instead of cleaving new sites at the boundary.

Thus, even though a multi-spider system adds spiders at the origin as fast as possible to prevent the leading spiders from moving too far backwards into the product sea, all multi-spider systems eventually decay to diffusion. This is the same qualitative behavior exhibited by single spider systems. However, multi-spider systems move superdiffusively over significantly longer times, and even when $r = 1.0$. They also reach a higher peak value of $\alpha(t)$. The superdiffusive properties of the multi-spider model can be quantified by examining the following:

- $\alpha_{\max} = \max_{t \geq 0}(\alpha(t))$, the peak instantaneous value of $\alpha(t)$, which should satisfy $1 \leq \alpha_{\max} \leq 2$;
- $t_{\alpha_{\max}} = \text{argmax}_{t \geq 0}(\alpha(t))$, the time at which the peak of $\alpha(t)$ is reached;
- and t_d, the time at which $\alpha(t)$ drops below the threshold of 1.1, and enters the diffusive phase.

The estimates of these quantities are given in Table 3. The results show that $\alpha_{\max}$ and t_d generally increase with decreasing r. Furthermore, the walkers with $r = 0.005$ have peak $\alpha(t)$ values above 1.9 and remain superdiffusive over times more than 6 orders of magnitude larger than the mean leg-product residence time.[2] Hence, for finite distances and times relevant to most transport processes the multi-spider model can achieve significant superdiffusive motion, and with small r values becomes nearly ballistic for significant spans of time and distance.

A further method of characterizing the transport behavior of multi-spider systems is to look at their effective instantaneous diffusion rate which (in 1D) is defined as

$$\widetilde{D}(t) = \text{msd}(t)/2t. \tag{15}$$

This is arrived at by setting $\alpha = 1$ in Eq. 6. The value of $\widetilde{D}(t)$ can be thought of as the diffusion rate a simple diffusing particle would need to have the same mean squared displacement as the spider system at time t. Hence, greater values of $\widetilde{D}(t)$ correspond to faster transport systems. Figure 7 shows $\widetilde{D}(t)$ for the multi-spider systems. While initially the spiders with lower r have larger $\widetilde{D}$ values, eventually the spiders with the smallest r values are superior.

4.2 Comparison with single spiders

The multi-spider systems can be directly compared with the single spiders to understand exactly how useful the additional interior spiders are for transport. Figure 8 shows the results of comparing the msd(t) for a single spider, and the leading spider of the multi-spider model, both with $r = 0.05$. There is a significant transport advantage for the multi-spider system. Furthermore, Fig. 9 shows the estimate of $\alpha(t)$ for these two systems, and the leading spider of the multi-spider system maintains a higher value of

[2] The value of $k_{\overline{P}}$ is a free parameter in the model. We choose time units so that rate $k_{\overline{P}}$ is normalized to 1, hence all time units are measured relative to $1/k_{\overline{P}} = 1$.

Table 3 Properties of the MSD and the superdiffusive regime defined by $\alpha(t) > 1.1$ for R_s

	Multi-spider r value						Single-spider r value	$k = 1$ spider r value
	1.0	0.5	0.1	0.05	0.01	0.005	0.05	1.0
$\alpha_{\max}$	1.38	1.37	1.63	1.73	1.87	1.93	1.43	1.41
$t_{\alpha_{\max}}$	9.03×10^1	1.03×10^2	8.60×10^1	1.50×10^2	2.83×10^3	1.02×10^4	2.17×10^2	2.71×10^1
t_d	2.43×10^5	2.75×10^5	2.10×10^5	1.89×10^5	1.02×10^6	3.31×10^6	2.52×10^4	1.14×10^5

Results are compared for the multi-spider model as well as the single spider model (Sect. 4.2) and the $k = 1$ spiders which are simple random walkers (Sect. 6)

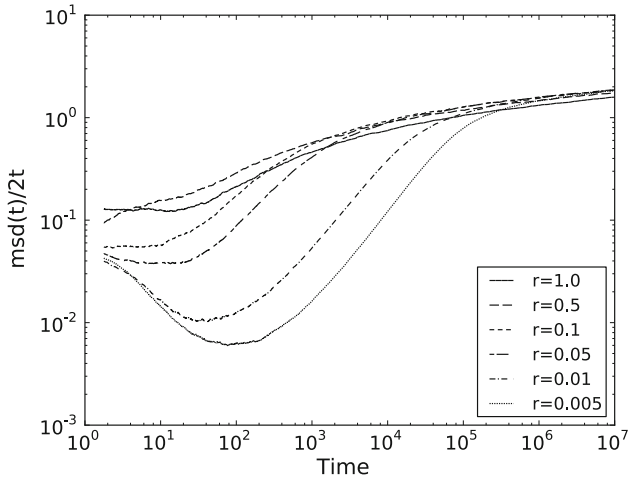

Fig. 7 Effective diffusion rate ($\widetilde{D}(t)$) for R_s

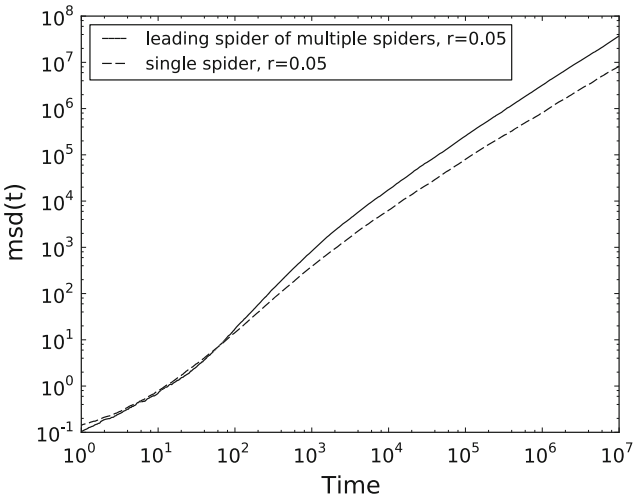

Fig. 8 Mean squared displacement for the leading spider R_s in the multi-spider model versus a single AK spider

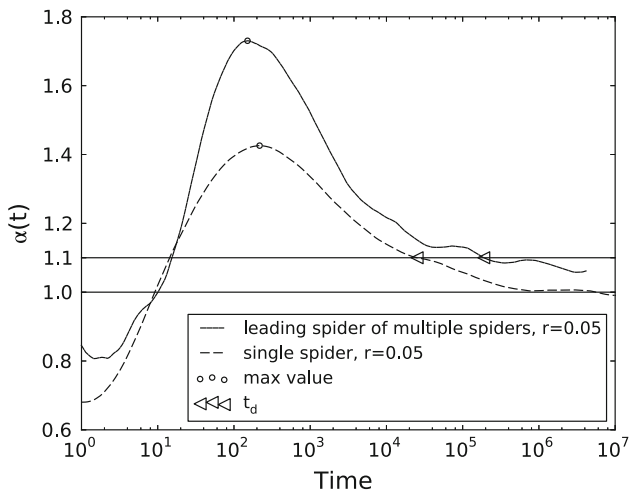

Fig. 9 Finite difference approximation of $\alpha(t)$ for the leading spider R_s in the multi-spider model versus a single AK spider

$\alpha(t)$ at all times, and significantly longer superdiffusive period. The values of $\alpha_{\max}$ and t_d are summarized in Table 3, and the multi-spider system is superior in both measurements. Finally, we compare the first passage times for the single versus multi-spider models in Fig. 10. The mean first passage time $\langle \text{fpt}(d) \rangle$ is the average time for the leading spider to first visit a site at a distance d from the origin. At large times the multi-spider systems have a large advantage in this key transport statistic. Overall, the comparison with the single AK spider shows that for distances <3,000 sites from the origin the leading spider of the multi-spiders model reaches unvisited sites up to 5.25 times faster than a single AK spider.

5 Asymptotic diffusion in the multi-spider model

In comparison with a single spider, the simulation results in Sect. 4 show that multi-spider systems exhibit larger values for $\widetilde{D}$, $\alpha_{\max}$, and t_d—all essential measures of transport efficiency. However, multi-spider systems still eventually decay to diffusion despite the unlimited supply of spiders injected at the origin. By analogy with the single spider model (Sect. 2.2), this implies that the effective size of the product sea as seen by the leading spiders is not constant. As the effective product sea grows, the leading spiders spend progressively less time at the boundary in the B state

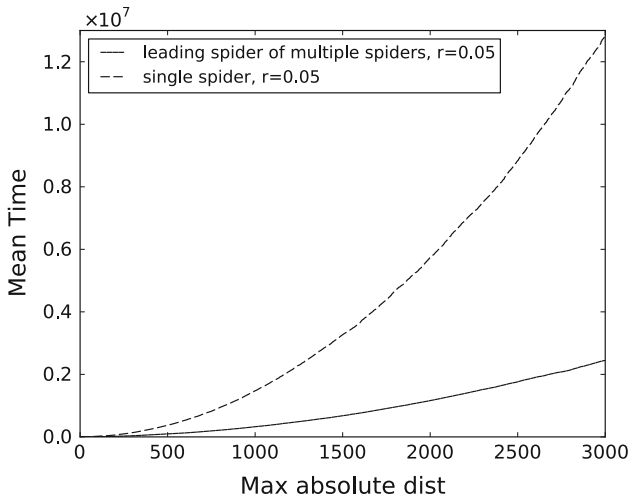

Fig. 10 Comparison of the first passage time of the leading spider R_s in the multi-spider model versus a single AK spider

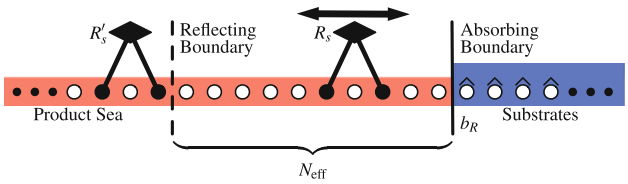

Fig. 11 The effective size of the product sea (N_{eff}) as seen by leading spider R_s is the area between next-leading spider R'_s and the right boundary b_R

where they move ballistically, and more time in the diffusive D state where they move over the product sea. This leads to a value of $\alpha(t) \to 1.0$, as $t \to \infty$, and the leading walkers are effectively diffusing. The origins of this effect can be understood in detail by examining the effective size of the product sea (Sect. 5.1), the number of released spiders (Sect. 5.2), and their spatial distribution (Sect. 5.3).

5.1 Effective size of the product sea

In 1D, spiders cannot move past each other, and thus the motion of the leading spiders R_s and L_s is constrained by the presence of their neighboring spiders. In particular when $S \geq 3$ we can define the next-leading spiders, R'_s and L'_s as

$$R'_s = \max_{\substack{1 \leq i \leq S \\ i \neq R_s}} (\mu(F_i)) \tag{16}$$

and

$$L'_s = \min_{\substack{1 \leq i \leq S \\ i \neq L_s}} (\mu(F_i)). \tag{17}$$

When $S \geq 4$, $L'_s \neq R'_s$, and the remaining $S - 4$ spiders are called the interior spiders. The importance of the next-leading spiders, R'_s and L'_s, is that they define the effective size of the product sea as seen by the leading spiders. Without loss of generality we focus only on the rightmost spiders R_s and R'_s and define

$$\langle N_{\text{eff}}(t) \rangle = \langle \max \left(F_{R'_s}(t) \right) + 1 - b_R(t) \rangle, \tag{18}$$

where the system state at time t is given by $X(t)$ from Eq. 9, and $b_R(t)$ is the right boundary for that state as defined in Eq. 8. Figure 11 illustrates what N_{eff} is for a particular state X. The choice of name for $\langle N_{\text{eff}}(t) \rangle$ is meant to correspond to Antal and Krapivsky's $\langle N(t) \rangle$ (Antal and Krapivsky 2007), which is the mean number of sites cleaved by a single spider system at time t. It has been shown for single spiders that $\langle N(t) \rangle = \Theta(\sqrt{t})$ (Antal and Krapivsky 2007), and that this implies that the time to leave the diffusive metatstate $\langle \tau_D(t) \rangle = \Theta(\sqrt{t})$ (Semenov et al. 2011). Since $\langle \tau_D(t) \rangle$ grows with time, and $\langle \tau_B(t) \rangle$ does not, single spiders eventually spend almost all their time diffusing in the D state and hence their motion is asymptotically diffusive.

The relation of $\langle N(t) \rangle$ with $\langle \tau_D(t) \rangle$ is based on the mathematics of the mean time for a random walker to escape an interval of size N with two absorbing boundaries. This gives the time for a walker to leave the product sea and return to the boundary. In the case of the multi-spider system, N_{eff} is also meant to represent the size of the region of products to escape from; however, it has one reflecting boundary at $\max \left(F_{R'_s} \right)$ and one absorbing boundary at b_R. The problem of escape from a region with one reflecting and one absorbing boundary is equivalent to escape from a region of twice the size with two absorbing boundaries (Fig. 12). Hence, we note the relation:

$$\langle N_{\text{eff}}(t) \rangle = \langle N(t) \rangle / 2. \tag{19}$$

Further analysis of this relationship is deferred to Sect. 7. However, the importance of N_{eff} can be understood simply—if $\langle N_{\text{eff}}(t) \rangle$ increases with time, then because $\langle \tau_D(t) \rangle = \Theta(\langle N_{\text{eff}}(t) \rangle)$, the leading spider R_s must eventually move diffusively. This is indeed the case for all values of r, as shown in Fig. 13. In this figure we used the Levenberg-Marquardt algorithm (Press et al. 2002) to fit power laws to the estimates of $\langle N_{\text{eff}}(t) \rangle$. We see that, interestingly, the exponents are close to 0.5—exactly as with single spiders.

Thus, $\langle \tau_D(t) \rangle$ for R_s also grows with time and therefore leads to asymptotic diffusion. However, in the multiple spider model the effective size of the product sea is much smaller than the total number of products ($\langle N_{\text{eff}}(t) \rangle \ll |P(t)|$) because most of the product sea is filled with other spiders, whereas in the single spider model $\langle N(t) \rangle = |P(t)|$. Thus, R_s in the multi-spider model remains superdiffusive for much higher values of $|P|$ than a single spider does. Fig. 14 compares the effective

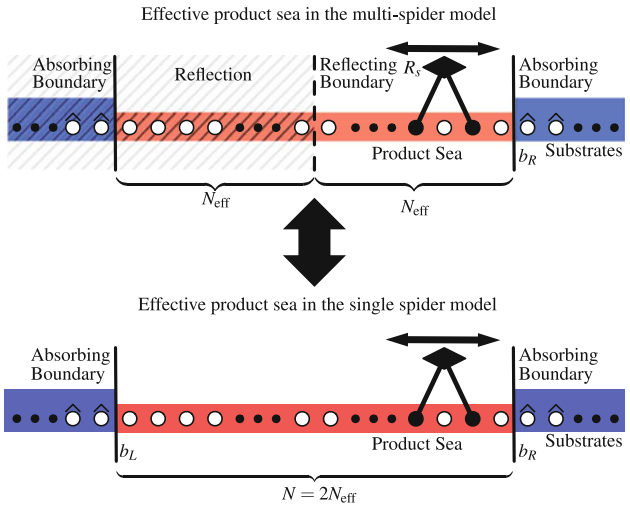

Fig. 12 The problem of escape from an area of size N_{eff} with one reflecting and one absorbing boundary is equivalent to the problem of escape of a single spider from a region of size $N = 2N_{\text{eff}}$ with two absorbing boundaries

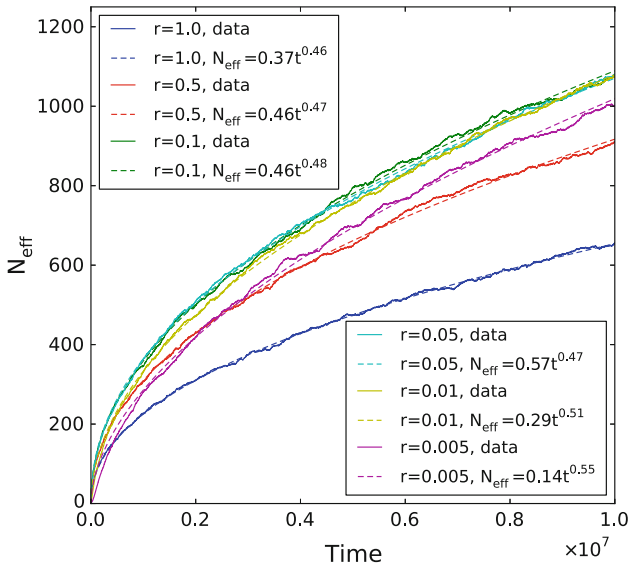

Fig. 13 The effective size of the product sea $\langle N_{\text{eff}}(t)\rangle$ grows with time, and hence leads to asymptotically diffusive motion for the multi-spider model

size of the product sea of the multi-spider model with the number of products of the AK model. While both $\langle N(t)\rangle$ and $\langle N_{\text{eff}}(t)\rangle$ grow with time, the single spider sees a much larger product sea, which explains the results of Sect. 4.2.

5.2 Number of released spiders

With injection rate $\lambda = \infty$, spiders in the multi-spider model are released at $I = \{0,1\}$ *whenever possible*, yet the presence of other spiders in the sites 0 and 1 prevents release, and so keeps the total number of spiders, S, finite.

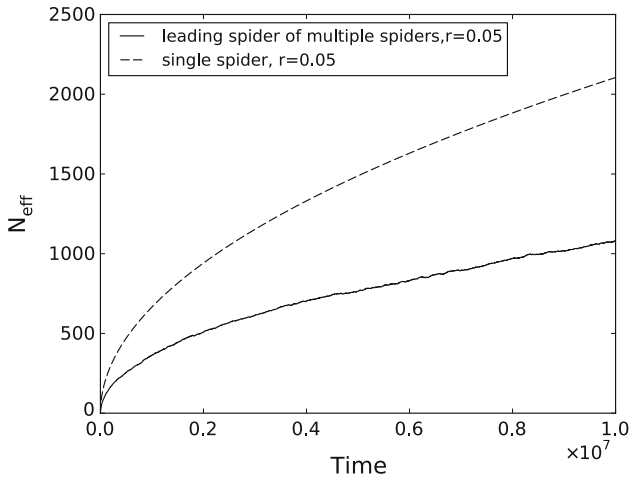

Fig. 14 The effective size of the product sea ($\langle N_{\text{eff}}(t)\rangle$) as seen by R_s in the multi-spider model versus the effective size of the product sea ($\langle N(t)\rangle$) for a single walker in the AK model

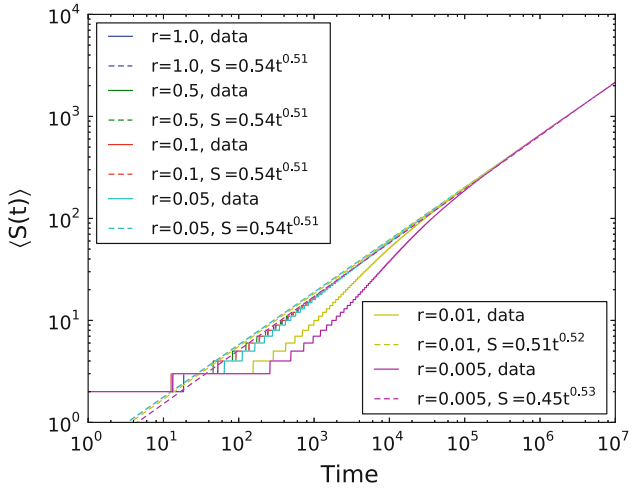

Fig. 15 Mean number of released spiders, $\langle S(t)\rangle$; the log-log scale is necessary to exhibit the differences at early times

Hence, $S(t)$ is a random variable giving the number of spiders released by time t. Figure 15 shows our estimates for $\langle S(t)\rangle$, for each studied value of r. Again we used the Levenberg-Marquardt algorithm to fit power laws, and observe approximate exponents of 0.5. Interestingly, $\langle S(t)\rangle$ appears to be dependent on r only initially, whereas at later times the values of $\langle S(t)\rangle$ for all r are nearly identical. Thus, the release of spiders, which occurs at the origin and away from the substrates at the boundaries, is independent of r, which limits the total number of released spiders regardless of how fast the leading spiders move.

5.3 Spatial distribution of spiders

Until now we have focused mainly on the position of the leading spiders R_s and L_s, but the behavior of the interior

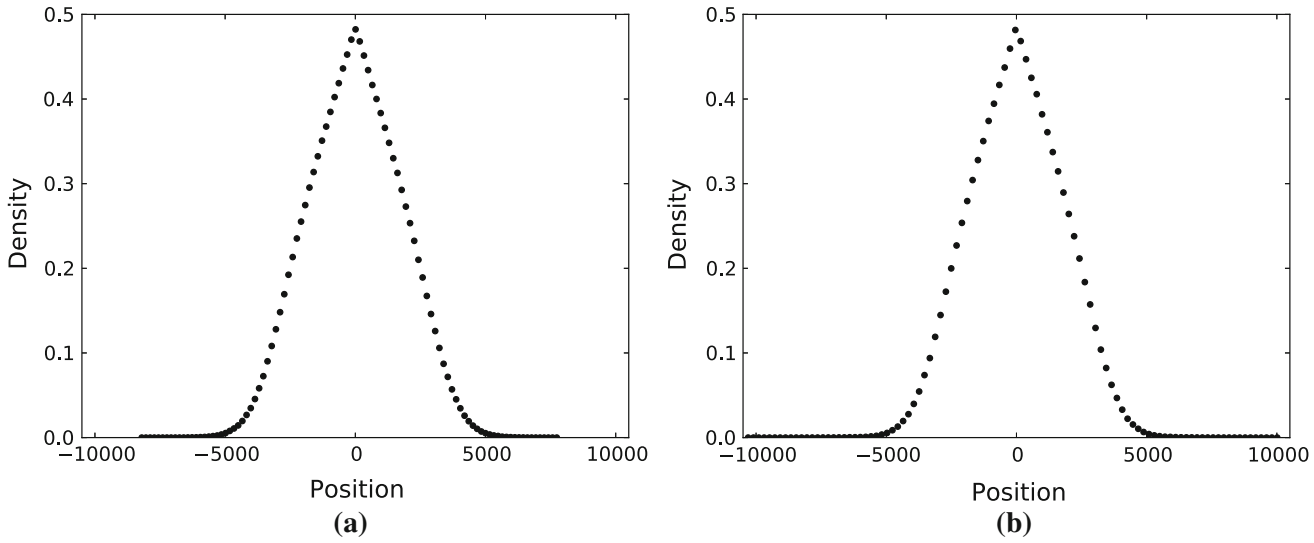

Fig. 16 Mean spider density at t_{max}, for $r = 1$ (**a**), and $r = 0.05$ (**b**)

spiders controls the release of spiders at the origin and the effective product sea size near the boundary. At any time t, we measure the density of spiders using a histogram with 100 equally spaced bins over the maximum positions obtained by any spider in any simulation trace at that time. Each bin with n sites can contain at most $n/2$ spiders, hence the maximum density for each bin is 0.5. Figure 16 shows the density of spiders at $t_{max} = 10^7$ for $r = 1$ and $r = 0.05$. The density of spiders near the origin is approximately the same in both cases and is nearly equal to the 0.5 maximum possible density. This explains why $\langle S(t) \rangle$ for large t is nearly the same for all r values. The sites near the origin are very densely packed for any r value and the passive addition of spiders is not presented with many opportunities to add new spiders even when the injection rate is infinite.

The density of spiders falls off nearly linearly away from the origin, until approximately distance 4,000 (at $t_{max} = 10^7$), where densities for both r values gradually transition to long tails with nearly 0 density. Essentially, the only difference between the densities for $r = 1$ and $r < 1$ is at the tails. The tails for $r = 0.05$ are much longer, corresponding to the greater msd(t_{max}) value observed for this r value. This is to be expected as only the leading spiders R_s and L_s ever see a substrate, and all other spiders only move over products. Thus the rate r only affects the motion of the leading spiders and those spiders near to the leading spiders that have comparatively more space to diffuse in. The vast majority of the interior spiders are too far from the leading spiders to see the effects of the r value. Hence, the distribution of spiders away from the boundaries is nearly identical for $r = 1$ and $r < 1$.

This similarity in densities of interior spiders is present at all times, as can be seen in Fig. 17, which shows the evolution of these densities with time. For both $r = 1$ and $r = 0.05$, the densities drop off linearly around the origin, until a critical point where they transition gradually to the near-zero density tails. The tails of the $r = 0.05$ spider density remain longer as expected based on the MSD results of Fig. 5, but the evolution of the interior spider density is nearly independent of r.

5.3.1 *Distribution of spider strides*

Spiders with $k = 2$, $s = 2$ only have two possible foot patterns: either both of their legs are together, or both are apart (Sect. 2.1). The together and apart patterns can be called the two possible *strides* of a spider. A single spider is equally likely to be in either of the two strides. However, the spiders in the multi-spider model show a curious distribution of leg patterns. Figure 18 shows the distribution of spiders in each of the two strides at time t_{max}, and again the results are remarkably similar for both $r = 1$ and $r < 1$. The high density of spiders near the origin leads to a very strong bias towards the together stride.

This can be considered an emergent phenomenon that arises as a means to increase spider packing close to the injection source. Spiders in this high density region rarely get an opportunity to spread their legs into the apart stride because both neighboring sites are almost always occupied. Also of note, at the distances where the linear decrease in spider density is no longer apparent, the distributions of strides becomes equal again. This equality of stride distribution indicates that the spiders are no longer experiencing the extreme exclusionary pressure observed near the injection site. Instead, the spiders on the periphery are able to act more like single spiders, which have an equal

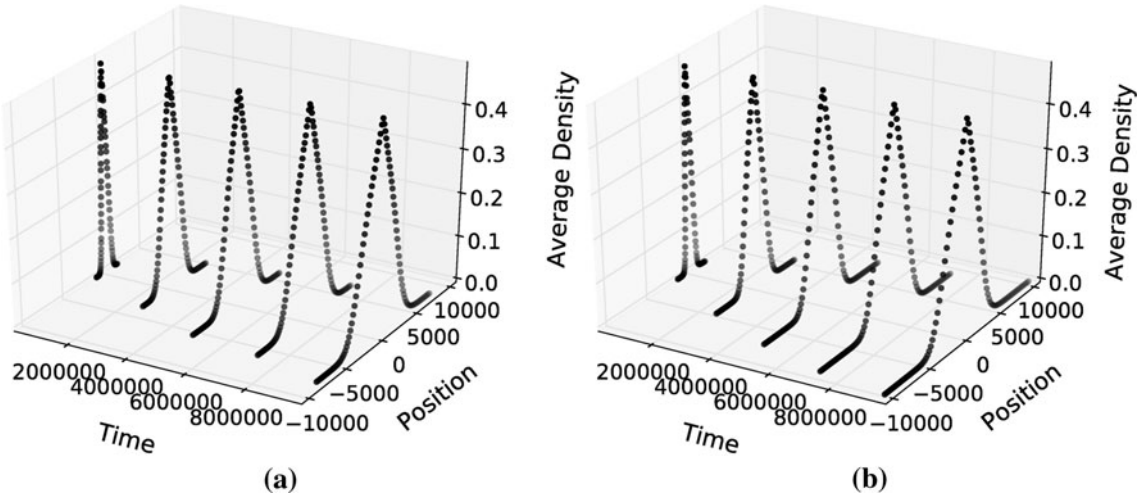

Fig. 17 Evolution of mean spider density through time, for $r = 1$ (**a**) and for $r = 0.05$ (**b**)

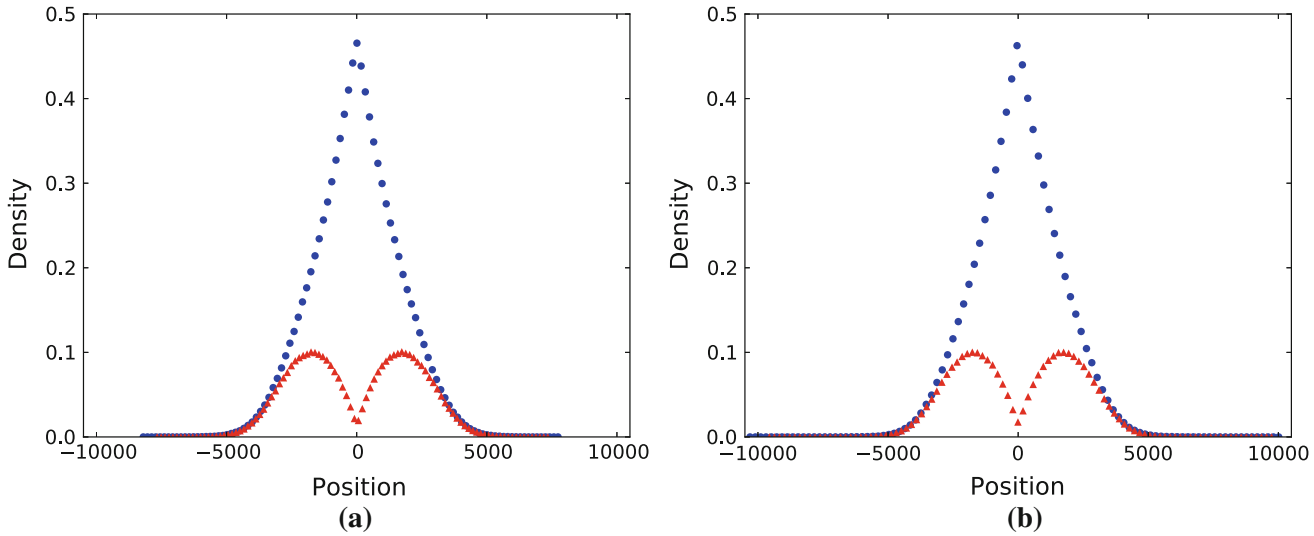

Fig. 18 Mean density of spiders in each of the together (*blue circles*) and apart (*red triangles*) strides at $t_{\{\max} = 10^7$, for $r = 1$ (**a**) and for $r = 0.05$ (**b**)

distribution in strides. These effects are again apparent at all time scales, as seen in Fig. 19.

5.3.2 *Density of leading spiders*

Unlike the interior spiders, which never see a substrate, the leading spiders L_s and R_s are strongly affected by the enzymatic rate r. When spiders are in the boundary metastate (Sect. 2.2), they move ballistically away from the origin, and the smaller the value of r, the less chance they have of exiting the boundary state and returning to the diffusive D state. Figures 20 and 21 show the probability distribution of $\mu(R_s)$ (the leading spiders location) for both $r = 1$ spiders and $r = 0.05$ spiders. Particularly at the shorter times in Fig. 21, there is a distinct difference in the distributions shape, with the $r < 1$ distributions having much longer tails, and distinctly non-Gaussian shape. The mean of the distributions is the msd(t), reported in Sect. 4.1.1, which grows much faster for the $r < 1$ multi-spider systems than for $r = 1$. However, the complete distributions shown in Figs. 20 and 21 reveal more information, particularly that the tails of the distribution are much shorter on the left than the right. This arises from the exclusionary pressures exerted by the next leading spider R'_s. However, the results of Sect. 5.1 show that despite this exclusionary pressure, the distance between the two leading spiders $\langle N_{\text{eff}}(t)\rangle$ continues to increase as $\sqrt{t}$ regardless of the value of r. Hence, in the distributions at $t_{\max}$ in Fig. 20, there is less distinction between the $r = 1$ and $r < 1$ walkers.

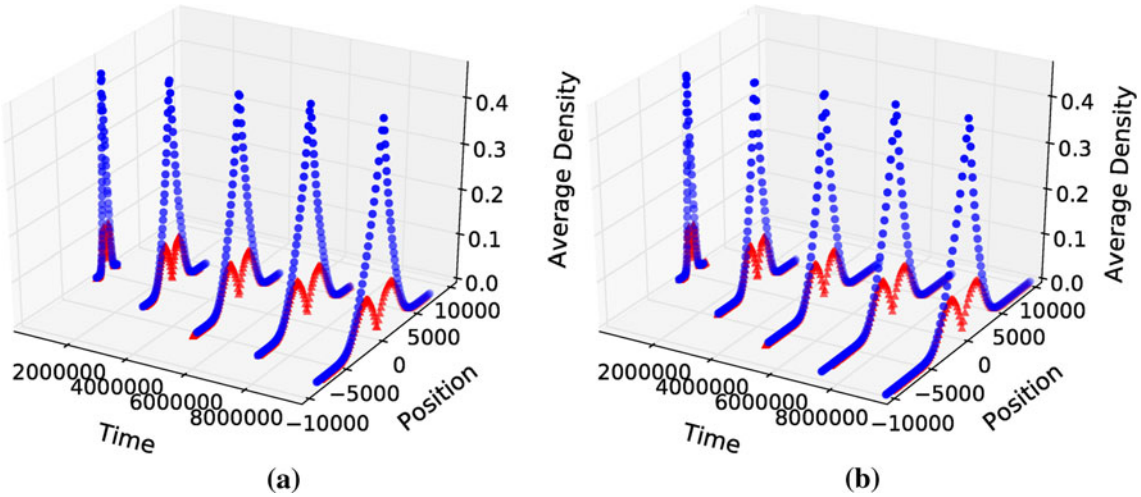

Fig. 19 Average density for spiders with legs together (*blue circles*) and apart (*red triangles*) plotted at several instants, for $r = 1$ (**a**) and for $r = 0.05$ (**b**)

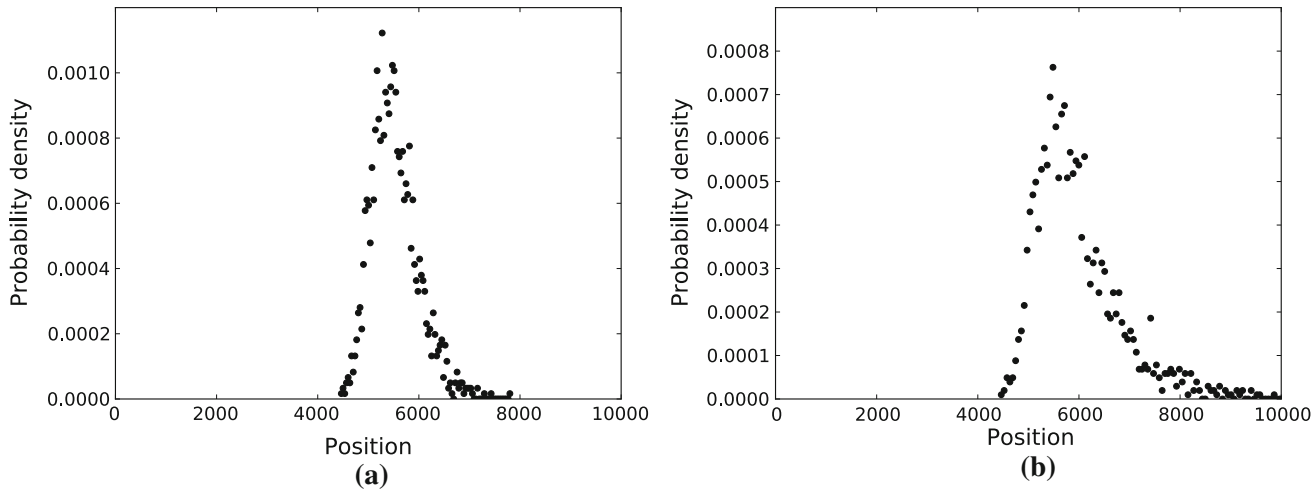

Fig. 20 Average density of the leading spider at $t_{\{\max}$, for $r = 1$ (**a**) and for $r = 0.05$ (**b**)

6 Importance of multi-pedal gaits for transport

Many molecular walkers, including the natural motors kinesin and dynein, are multivalent—they have two (or more) attachment sites. Interestingly, it has been shown that in the AK spider model, the superdiffusive effects are only present when the number of legs $k \geq 2$. Without the constraints imposed by multiple legs the residence time-bias at the boundary when $r < 1$ does not lead to a bias in motion towards substrates.

The multi-spider model has two potential sources of bias to cause superdiffusive motion of the leading spiders: the residence time bias at the boundary when $r < 1$, and the effective bias caused by the exclusionary pressure of the interior spiders. We know that the multi-spider systems are transiently superdiffusive even when $r = 1$ due to the exclusionary pressure, but what happens to their collective behavior when they have only a single leg? In fact when $k = 1$ and $r = 1$ an AK spider is equivalent to an ordinary random walker that moves left and right with rate 1. Thus, we measured msd(t) for the leading walker of the multi-spider model with $k = 1$ and $r = 1$. The values for msd(t) are compared with the multi-spiders model with $k = 2$ and $r \in \{1.0, 0.1\}$, and shown on a log-log scale in Fig. 22, and the corresponding values of $\alpha(t)$ are shown in Fig. 23. The $k = 1$ walkers do exhibit transient superdiffusive behavior, but their values of $\alpha_{\max}$ and t_d are surpassed by $k = 2$ spiders when $r < 0.1$, as summarized in Table 3. Spiders with $k = 1$ achieve maximum msd(t) when $r = 1$ (Antal and Krapivsky 2007, Antal et al. 2007), so by using $r = 1$ in our comparison we are comparing with the most efficient single-legged spiders possible.

It is, however, necessary to make an adjustment of scales to correctly compare the msd(t) values between $k = 2$ and $k = 1$

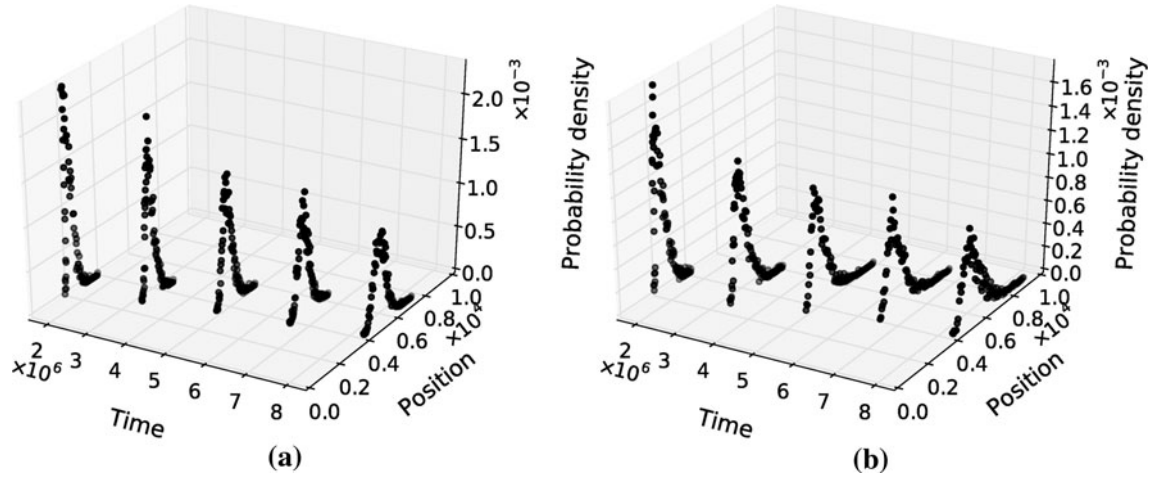

Fig. 21 Average spider density of the leading spider plotted at several instants, for $r = 1$ (**a**) and for $r = 0.05$ (**b**)

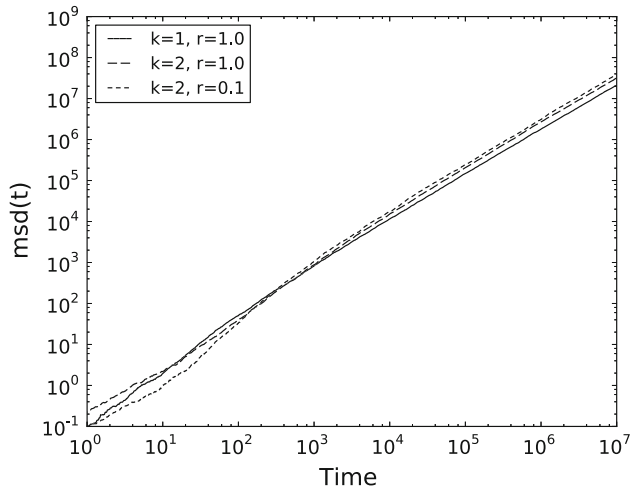

Fig. 22 Comparison of msd(t) for the leading spider R_s in multi-spider simulations versus the $k = 1$ multi-spider model (with corrected diffusion constant of $D = 0.5$.)

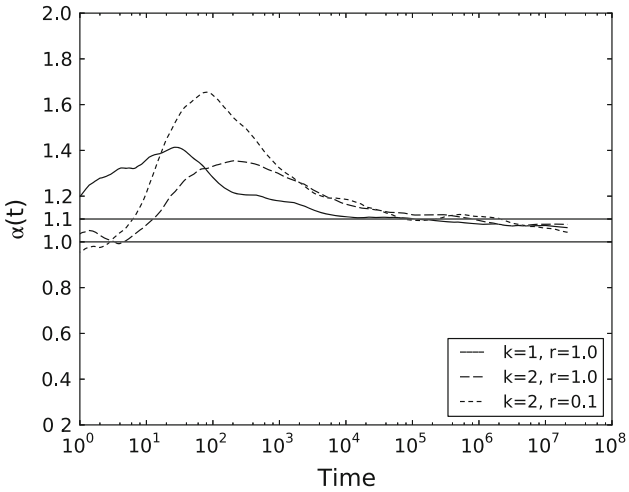

Fig. 23 Comparison of finite difference approximation of $\alpha(t)$ for the leading spider R_s in multi-spider simulations versus the $k = 1$ multi-spider model (with corrected diffusion constant of $D = 0.5$.) Horizontal lines show the threshold for ordinary diffusion at $\alpha = 1$ and our defined threshold for superdiffusion at $\alpha = 1.1$

walkers. Since the position of a spider is defined as the mean of its attached leg positions, the $k = 2$ spiders move by only distance 0.5 with each step, in contrast to the $k = 1$ spiders which move by distance 1. Thus, in the analysis of $k = 1$ spiders shown in Figs. 22 and 23, the $k = 1$ spiders move over a lattice with site spacing 0.5. In essence this correction can be thought of as adjusting the diffusion constant of the $k = 1$, $r = 1$ walkers which have $D = 1$ to that of the $k = 2$, $r = 1$ walkers which have $D = 0.5$.

7 Analysis of maximum product sea size

Simulation results presented in Sect. 4.1.1 suggest that the leading spider R_s moves diffusively in the long time limit with the value of $\alpha(t_{\max}) \approx 1$. Section 5.1 showed that this happens because the mean effective size of the product sea as seen by R_s, $\langle N_{\text{eff}}(t)\rangle$, grows with time approximately as $\sqrt{t}$. Hence, the duration of the D states $\langle \tau_D(t)\rangle$ also grows with time, leading to asymptotically diffusive motion. Furthermore the effective product sea size N_{eff} can also be understood as being a function N, the number of sites cleaved. Figure 24 shows simulation estimates for $\langle N_{\text{eff}}(N)\rangle$, which at times close to $t_{\max}$ is almost linear. Thus, while the leading spider is cleaving sites at the boundary, the interior spiders are not following closely enough and the leading spider sees an increasingly large effective product sea. If a multi-spider system were to keep the leading spider superdiffusive as $t \to \infty$, it would have to ensure that $\langle N_{\text{eff}}(N)\rangle$ does not grow

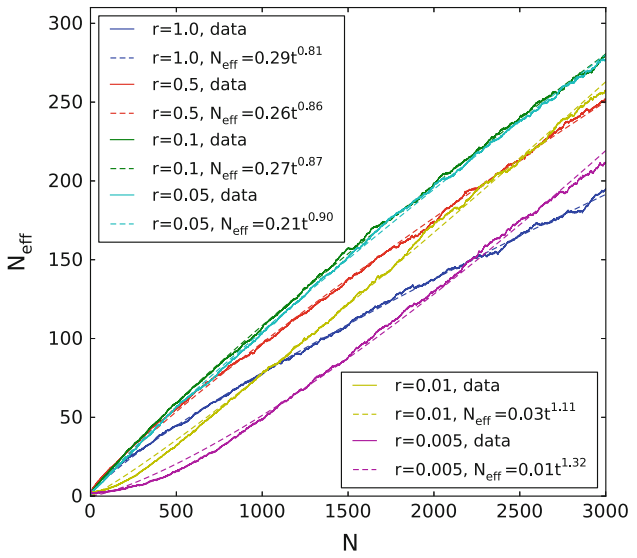

Fig. 24 Size of the effective product sea $\langle N_{\text{eff}}(N)\rangle$ as a function of the number of visited sites N

too fast. The asymptotic bound that ensures this property can be found analytically.

The expected exit time for a random walker from an interval (0,M) with two absorbing boundaries at 0 and M is

$$\langle T_e(x)\rangle = \frac{x(M-x)}{2}, \tag{20}$$

where x is the starting position of the walker. As shown in Fig. 12 and explained in Sect. 5.1, the expected exit time from an interval with one absorbing and one reflecting boundary is the same as exit time from a interval with two absorbing boundaries of twice the size. Furthermore, when a spider moves over a region of product sites, its body position $\mu(F)$ moves like a simple random walker with a step size of 1/2.

When at time t the R_s spider moves off the boundary and into the D state, it enters a product sea of expected size $\langle N_{\text{eff}}(N)\rangle$ with one absorbing and one reflecting boundary. The expected time to exit this interval is the expected duration of the D-state, τ_D. This can be found by using Eq. 20 with $M = 4\langle N_{\text{eff}}(N)\rangle - 5$ and $x = 4\langle N_{\text{eff}}(N)\rangle - 8$, which gives

$$\langle \tau_D(N)\rangle = \langle T_e\rangle = \frac{3(4\langle N_{\text{eff}}(N)\rangle - 8)}{2}. \tag{21}$$

From Antal and Krapivsky (2007), the average time interval during which the number of visited sites grows from $N+3$ to $N+4$ is

$$\langle \tau_N\rangle = \frac{1}{r} + \frac{1+r}{2+r}\langle T_e\rangle, \tag{22}$$

and the expected time to visit $N+3$ sites is

$$\langle T(N)\rangle = \sum_{i=0}^{N-1}\langle \tau_N\rangle. \tag{23}$$

Thus, we can write $\langle N_{\text{eff}}(N)\rangle$ to be a function of N, and by substituting Eq. 21 into the sum in Eq. 23, we obtain

$$\langle T(N)\rangle = \frac{N}{r} + \frac{1+r}{2+r}\sum_{i=0}^{N-1}\frac{3(4\langle N_{\text{eff}}(i)\rangle - 8)}{2}. \tag{24}$$

Equation 24 shows that if $\langle N_{\text{eff}}(N)\rangle = \Theta(N)$, as Fig. 24 suggests, then $\langle T(N)\rangle = \Theta(N^2)$, which corresponds to diffusive motion. Hence, in order for the leading spider to be superdiffusive as $t \to \infty$, we require $\langle T(N)\rangle = o(N^2)$, which implied $\langle N_{\text{eff}}(N)\rangle = o(N)$. Unfortunately, as Fig. 12 shows, this is not the case for the multi-spider model—to maintain superdiffusive motion asymptotically, we need a mechanism stronger than passive injection at the origin.

8 Discussion

Collective and cooperative behaviors are essential to the motion of many natural molecular motors and cellular transport systems, yet the incredible complexity of natural motor systems makes it difficult to discern what types of walker interactions are necessary or sufficient for useful transport behavior. In this work we begin to address these fundamental questions of nanoscale cooperation by investigating a much simpler model of walker motion based on the kinetic and mechanical properties of DNA-enzyme-based molecular spiders. The AK model of spider motion, while lacking in chemical detail, is able to encompass those features of spider motion that are necessary for superdiffusive motion of single spiders in 1D (i.e., irreversibility of substrate modification, multiplicity of legs, and a kinetic bias between modified and unmodified sites). These seemingly simple properties have previously been shown to lead to useful superdiffusive motion (Semenov et al. 2011). Following this bottom-up approach to the investigation of spider motion, we have analyzed the collective behavior of multiple identical spiders as they cooperate using only simple exclusionary interactions. Clearly, more complex interactions are possible, but we have shown that this single additional feature allows spider systems to move cargo in 1D superdiffusively over significantly longer times and distances than can be accomplished with a single spider system (Sect. 4.1.1). Multiple spiders with small values of r achieve higher values of $\alpha_{\max}$ and t_d than either single AK spiders (Sect. 4.2) or cooperative single-legged spiders (Sect. 6). However, in the asymptotic limit as $t \to \infty$, we find that $\alpha(t) \to 1$, and the leading spiders of the multi-spider model move diffusively for all values of r.

Analysis of the AK model shows that this asymptotic decay to diffusion is also a fundamental property of the single spiders, and previous work has shown that the

diffusive behavior results from the switching of single AK spiders between two metastates that partition the process into alternating diffusive (D) and boundary (B) periods. Spiders move diffusively over products in the D metastate, and ballistically away from the origin while they are attached to energy-rich substrates in the B state. However, the duration of the B periods $\langle \tau_B(t) \rangle$ is constant in time, while the duration of D periods $\langle \tau_D(t) \rangle = \Theta(\sqrt{t})$ grows with time because the sea of products that the spider cleaves out also grows with time, and it takes increasingly long for spiders to exit this energy-devoid product sea.

A simple idea motivated the multi-spider model: if the effective size of the product sea N_{eff} could be sufficiently limited, then it would prevent the $\langle \tau_D(t) \rangle$ from growing with time and hence let the spider move asymptotically diffusively. This ends up not being the case, and even with new spiders injected at the origin as fast as possible, without violating the exclusionary properties of spiders. We still found $\langle N_{\text{eff}}(t) \rangle = \mathcal{O}(\sqrt{N})$ for all values of r (Sect. 5.1). The reasons behind this can be understood from several perspectives presented in this work.

One way to understand this result is to note the number of spiders released with time was $\langle S(t) \rangle = \mathcal{O}(\sqrt{t})$ and largely independent of r, even with the injection rate $\lambda = \infty$ (Sect. 5.2). Under asymptotically superdiffusive motion of the leading spiders we would see the number of products cleaved $N(t) = \omega(\sqrt{t})$, and to fill this product sea would require $S(t) = \Theta(N(t)) = \omega(\sqrt{t})$, which is not achieved by the multi-spider model. Thus, we cannot seem to release spiders fast enough to support superdiffusion indefinitely. This failure can be partly understood by observing that the only spiders that actually get to attach to and cleave the energy bearing substrates are the leading R_s and L_s spiders. The other, interior spiders only ever walk on products. Thus, while there is some bias exerted on interior spiders by the exclusionary pressure of injected spiders near the origin, for the most part the motion of interior spiders is governed by diffusion. Hence, they do not move fast enough to get clear of the injection site at the origin to allow enough other spiders to be injected fast enough. Indeed, the density of spiders (Sect. 5.3) around the origin is nearly maximal, and also seemingly independent of r. Thus, it does not really matter how small the value of r is (and hence how much biasing energy is contained within substrates), because the interior spiders see none of that energy and their diffusive motion is hence independent of r. Yet, the motion of these interior spiders remains the limiting factor for the injection rate of the new spiders needed to assist the leading spiders by reducing the effective size of the product sea. Hence, no matter how fast the leading spiders are able to move initially, they will inevitably be hindered by the insufficiently fast dispersal of the energy-deprived interior spiders.

Additionally, the failure of the multi-spider system to limit the effective product sea size can be seen with the analytical approach of Sect. 7. This shows us that a spider system that can ensure that $\langle N_{\text{eff}}(N) \rangle = o(N)$ will allow asymptotically faster-than-diffusion transport. Future work will concentrate on understanding how spider systems can achieve these bounds on the effective product sea size, potentially by supplying energy to the system from an external source. After all, the lack of energy available to the interior spiders seems to be the limiting factor for the cooperative transport behaviors of the multi-spider model.

Despite these asymptotic results, it should be remembered that all practical nanoscale transport problems for which molecular walkers are applicable take place over finite times and finite distances and both single and multi-spider systems show potential for faster-than-diffusion transport for such applications. Other interesting applications of spiders which we are currently investigating include cooperative 2D behavior for transport, and other chemically plausible modes of interaction between spiders and surfaces that are more complex than the simple exclusionary processes examined in this work.

Acknowledgments We thank Paul L. Krapivsky for insights into the behavior of multiple random walkers with an infinitely strong source (Krapivsky 2012). This material is based upon work supported by the National Science Foundation under grants 0829896 and 1028238.

References

Antal T, Krapivsky PL (2007) Molecular spiders with memory. Phys Rev E 76(2):021121

Antal T, Krapivsky PL, Mallick K (2007) Molecular spiders in one dimension. J Stat Mech Theory Exp 2007(08):P08027

Badoual M, Jülicher F, Prost J (2002) Bidirectional cooperative motion of molecular motors. Proc Natl Acad Sci USA 99(10):6696–6701

Bortz AB, Kalos MH, Lebowitz JL (1975) A new algorithm for Monte Carlo simulation of Ising spin systems. J Comput Phys 17(1):10–18

Campas O, Kafri Y, Zeldovich KB, Casademunt J, Joanny JF (2006) Collective dynamics of interacting molecular motors. Phys Rev Lett 97:038101

Frey E, Parmeggiani A, Franosch T (2004) Collective phenomena in intracellular processes. Genome Inform 15(1):46–55

Hirokawa N, Takemura R (2005) Molecular motors and mechanisms of directional transport in neurons. Nat Rev Neurosci 6(3):201–214

Jülicher F, Ajdari A, Prost J (1997) Modeling molecular motors. Rev Mod Phys 69(4):1269–1281

Krapivsky PL (2012) Symmetric exclusion process with a localized source. arXiv:1208.3250 [Cond-Mat Stat Mech]

Lacasta AM, Sancho JM, Romero AH, Sokolov IM, Lindenberg K (2004) From subdiffusion to superdiffusion of particles on solid surfaces. Phys Rev E 70(5):051104

Lund K, Manzo AJ, Dabby N, Michelotti N, Johnson-Buck A, Nangreave J, Taylor S, Pei R, Stojanovic MN, Walter NG,

Winfree E, Yan H (2010) Molecular robots guided by prescriptive landscapes. Nature 465:206–210

Pei R, Taylor SK, Stefanovic D, Rudchenko S, Mitchell TE, Stojanovic MN (2006) Behavior of polycatalytic assemblies in a substrate-displaying matrix. J Am Chem Soc 128(39): 12693–12699

Press WH, Teukolsky SA, Vetterling WT, Flannery BP (2002) Numerical recipes in C++. Cambridge University Press, New York

Schliwa M, Woehlke G (2003) Molecular motors. Nature 422(6933):759–765

Semenov O, Olah MJ, Stefanovic D (2011) Mechanism of diffusive transport in molecular spider models. Phys Rev E 83(2):021117

Semenov O, Olah MJ, Stefanovic D (2011) Multiple molecular spiders with a single localized source—the one-dimensional case. In: DNA 17: Proceedings of the seventeenth international meeting on DNA computing and molecular programming. Lecture Notes in Computer Science, vol 6397, Springer, pp 204–216